Future reef growth can mitigate physical impacts of sea-level rise on atoll islands

Edward S Beetham, Paul S Kench, Stéphane Popinet

Future reef growth can mitigate physical impacts of sea-level rise on atoll islands

Edward Beetham [1,*], Paul S. Kench [1], and Stéphane Popinet [2,3]

[1] School of Environment, University of Auckland, Auckland, New Zealand

[2] Sorbonne Universités, UPMC Univ Paris 06, UMR 7190, Paris, France

[3] CNRS, UMR 7190, Institut Jean le Rond d'Alembert, Paris, France

*Corresponding author: Edward Beetham

e.beetham@auckland.ac.nz , +64 9 3737599x89917

Key points

- A static reef response to sea-level rise will decrease the contemporary influence of infragravity waves on coral reefs
- Vertical reef accretion with sea-level rise will protect islands from higher wave energy and dampen wave driven flooding volumes by 72%
- Significant adaptation is required for islands on the eastern rim of Funafuti Atoll to remain inhabitable beyond 2090 under RPC8.5

Abstract

We present new detail on how future SLR will modify nonlinear wave transformation processes, shoreline wave energy and wave driven flooding on atoll islands. Frequent and destructive wave inundation is a primary climate-change hazard that may render atoll islands uninhabitable in the near future. However, limited research has examined the physical vulnerability of atoll islands to future SLR and sparse information is available to implement process based coastal management on coral reef environments. We utilize a field-verified numerical model capable of resolving all nonlinear wave transformation processes to simulate how future SLR will modify wave dissipation and overtopping on Funafuti Atoll, Tuvalu, accounting for static and accretionary reef adjustment morphologies. Results show

This article has been accepted for publication and undergone full peer review but has not been through the copyediting, typesetting, pagination and proofreading process, which may lead to differences between this version and the Version of Record. Please cite this article as doi: 10.1002/2017EF000589

that future SLR coupled with a static reef morphology will not only increase shoreline wave energy and overtopping but will fundamental alter the spectral composition of shoreline energy by decreasing the contemporary influence of low frequency infragravity waves. '*Business-as-usual*' emissions (RCP 8.5) will result in annual wave overtopping on Funafuti Atoll by 2030, with overtopping at high tide under mean wave conditions occurring from 2090. Comparatively, vertical reef accretion in response to SLR will prevent any significant increase in shoreline wave energy and mitigate wave driven flooding volume by 72%. Our results provide the first quantitative assessment of how effective future reef accretion can be at mitigating SLR associated flooding on atoll islands and endorse active reef conservation and restoration for future coastal protection.

Key words

Atoll; Reef island; Sea-level rise; Wave transformation; Wave overtopping; Infragravity wave

1. Introduction

Future habitation on low-lying atoll islands is at risk from an increase in flooding and wave inundation associated with sea-level rise (SLR) and anthropogenic climate change [*Storlazzi et al.*, 2015]. As geological structures, coral islands are accumulations of reef-derived biogenic sediment deposited on atoll and platform reefs, with elevations rarely exceeding 2-3 m above mean sea-level (MSL) [*Woodroffe*, 2008; *McLean and Kench*, 2015]. Rising sea-levels are expected to result in larger waves at reef island shorelines, increasing the frequency and magnitude of wave generated flooding events [*Sheppard et al.*, 2005; *Quataert et al.*, 2015]. Wave inundation is a major concern for reef island communities, with negative impacts including physical damage to homes and critical infrastructure, destruction of food resources and contamination of freshwater reservoirs [*Connell*, 2003; *Lazrus*, 2012; *Lin et al.*, 2014; *Nurse et al.*, 2014]. Under contemporary conditions, wave overtopping on reef islands typically requires a large wave event coincident with highest tidal levels, a combination of factors that occurs every 2-3 years [*Merrifield et al.*, 2014]. However, more frequent wave overtopping associated with SLR will limit recovery time between events and may strain the coping capacity of island communities to a point that seriously compromises permanent habitation [*Barnett and Adger*, 2003; *Patel*, 2006].

Recent analysis of wave interaction with atoll reefs under SLR scenarios suggest that the tipping-point when islands may become uninhabitable will occur in a few decades, when runup under modal wave conditions exceeds the berm elevation [*Storlazzi et al.*, 2015]. However, previous investigations on the physical impact of SLR on reef islands omit two important negative feedback mechanisms that may offset the imminent threat of SLR for island communities. First, existing studies do not explicitly resolve the contribution of secondary wave motions (infragravity waves and wave setup) to island flooding or examine how these processes will respond to higher sea-level. Second, there has been no attempt to

quantify the effectiveness of future vertical reef accretion on mitigating the physical impact of SLR on reef islands.

Wave overtopping is influenced by three key wave processes, incident frequency sea-swell (SS) waves ($f > 0.04$ Hz), long period infragravity (IG) waves ($f \leq 0.04$ Hz) and water level setup shoreward of the breakpoint [*Merrifield et al.*, 2014]. Coral reefs are known to be highly effective at dissipating SS waves, reducing incident energy by as much as 97% before island shorelines [*Ferrario et al.*, 2014]. However, SS wave dissipation facilitates a transfer of energy to longer period (IG) wave motions which are consistently recognized as the dominant process influencing wave runup [*Beetham et al.*, 2016], overtopping [*Cheriton et al.*, 2016] and destructive flooding [*Roeber and Bricker*, 2015; *Shimozono et al.*, 2015] on reef shorelines. The presence of IG waves on coral reefs is associated with two key forming mechanisms: (1) the release of group-bound long waves when incident waves break [*Longuet-Higgins and Stewart*, 1962; *Masselink*, 1995] and (2) the propagation of dynamic setup arising from spatial variability in break-point location [*Symonds et al.*, 1982]. Both forcing mechanisms are associated with irregular incident wave groups and result in free-propagating long period waves on the reef flat [*Péquignet et al.*, 2014]. The development of IG waves with enough energy to overtop island shorelines requires a substantial reduction in SS energy through breaking and friction, which implies that IG energy may become less important at higher sea-levels if SS dissipation decreases [*Beetham et al.*, 2016]. Accurate predictions of wave driven flooding on reef coastlines must account for this nonlinear behavior between SS and IG frequency waves [*Roeber and Bricker*, 2015].

To date, studies that have examined the impact of SLR on wave transformation across coral reefs have assumed a static reef platform surface. However, many coral reefs are currently sea-level limited and future SLR will open accommodation space for vertical reef accretion [*Perry et al.*, 2012; *Woodroffe and Webster*, 2014]. Reef accretion represents a feedback to

existing interpretations of increased wave impacts and overtopping on islands that may provide a self-regulating mechanism to mitigate the physical impact of SLR on reef islands. To date such feedbacks have not been examined. The potential for future reef growth is the subject of continued speculation [*van Woesik et al.*, 2015]. Conventional wisdom suggests reef growth is likely to be compromised in many reef regions as a consequence of a global decline in coral cover, increased sea surface temperatures, ocean acidification and anthropogenic stresses [*Jackson et al.*, 2001; *Hughes et al.*, 2003, 2010; *Hoegh-Guldberg et al.*, 200fig. 7fig; *Hoegh-Guldberg*, 2014; *Aronson and Precht*, 2016]. However, recent studies have documented coral re-colonization across previously emergent reef flats due to SLR [*Brown et al.*, 2011; *Scopélitis et al.*, 2011] and land subsidence [*Saunders et al.*, 2015], providing evidence that locally some reefs may have capacity to vertically accrete and keep pace with future sea-levels. Indeed, recent field and modeling assessments show that sea-level constrained reefs in the western tropical Pacific are currently accreting in response to measured SLR and will continue to keep-up with future SLR at rates up to 6.1 mm/yr, even when negative effects of increasing sea-surface temperature are represented [*van Woesik et al.*, 2015]. Collectively, such studies suggest future reef growth responses are likely to vary between reef localities dependent on the antecedent condition of reefs and the severity of future pressures [*Kench et al.*, 2009; *Hamylton et al.*, 2014; *Perry et al.*, 2015]. In areas where reef accretion does occur, the effect on modifying wave processes and mitigating hazard risks to reef islands remain poorly resolved.

A third limitation of existing research on the physical impacts of SLR is the inability of wave transformation based studies to appropriately account for ongoing adjustments to island morphology as shoreline wave energy increases. Accounting for the morphodynamic impact of SLR on atoll islands is beyond the scope of this study but will be the focus of future research. The focus of this study is to resolve how SLR will modify the nonlinear wave

transformation processes that cause flooding and provide the boundary condition for island morphology change, accounting for static and accretionary reef responses. Recent advances in numerical modeling have developed phase-resolving techniques capable of accurately resolving water level motions associated with SS waves, IG waves, wave setup, runup and overtopping on coral reefs, providing an unprecedented ability to represent nonlinear wave transformation on morphologically complex reef environments [*Roeber and Cheung*, 2012; *Roeber and Bricker*, 2015; *Beetham et al.*, 2016]. This study is focused on Fatato Island, Funafuti Atoll, Tuvalu where previous research was done to evaluate wave transformation outputs from a fully nonlinear Boussinesq model against field measurements [*Beetham et al.*, 2016]. In this study, the same model was utilized to simulate wave transformation, runup and overtopping on Fatato with incremental SLR and variable reef response morphologies. Results are used to explore how long islands on the eastern rim of Funafuti will remain inhabitable before frequent inundation may compromise human occupation. This approach does not account for adjustments to island morphology and therefore assumes that ongoing habitation requires islands to maintain their current morphology.

2. Field setting

Fatato is located on the south-eastern rim of Funafuti Atoll and is comprised of sand and gravel size material, with a morphology representative of many high energy 'motu' islands throughout the Pacific Ocean, including neighboring island Fogafale, where approximately 6,000 people live (Fig. 1). Funafuti is located inside a SLR hotspot, where MSL increased by 0.3 m between 1950 and 2009 (5.1 mm yr^{-1}) [*Becker et al.*, 2012]. The atoll has been a focus for numerous studies examining climate change vulnerability [*Farbotko and Lazrus*, 2012; *Lazrus*, 2012; *Kench et al.*, 2015; *McCubbin et al.*, 2015] but existing research has not considered how increasing sea-level (SL) will change the physical processes that contribute to wave driven flooding. The ocean facing reef flat adjacent Fatato Island is approximately

100 m wide and the offshore reef slope is approximately 23.5°. Conglomerate platform and cemented rubble protrude seaward from the island base, with the beach toe elevated 0.39 m above MSL. The model transect from Fatato Island that was used in these experiments is representative of the typical topography of many islands on the eastern rim of Funafuti Atoll. The ocean shoreline has a steep gravel beach face (12° gradient) with a berm elevated 3.5 m above MSL (4.3 m above the central reef flat). The beach face and island are comprised entirely of calcium carbonate sediment derived from physical breakdown of the reef framework. Mean grain size on the beach face is 73 mm, with most clasts within the pebble or cobble size fractions, although boulder size clasts are scattered throughout the island and small sand pocks do exist on the beach face. Fatato Island is 80 - 90 m wide, with a basin in the center and a ridge on the lagoon shoreline (Fig. 1d).

The eastern reef flat on Funafuti Atoll is currently intertidal, with the outer reef flat elevated approximately 0.3 m above spring low tide levels. The potential for coral colonization and therefore vertical accretion on the reef flat will increase when SLR results in permanent submergence of the contemporary reef. Detailed reef drilling records show that the reef flat at Funafuti accreted by 26.4 m during the Holocene, at a mean rate of 5.0 mm/yr [*Ohde et al.*, 2002]. Two hypothetical reef growth morphologies were used in this research, based on an understanding of morphodynamic zonation of wave exposed reefs [*Hopley*, 2011; *Hamylton et al.*, 2014]. The first morphology concentrates reef accretion at the outer reef flat, representing a concentration of coral near the reef edge or the development of a prominent coralline algae and rubble ridge formation [*Guilcher*, 1988], with limited coral cover on the inner reef (Fig. 2). The second morphology applies a near-uniform level of reef accretion across the reef flat, representing coral colonization or sedimentary infill on the inner reef flat. Maximum elevation for both morphologies is at the same elevation as the SLR adjusted

spring low tide level (Fig. 2). Both reef accretion morphologies assume no change to the volume of island sediment.

3. Methods

3.1 Reef and island topography

A laser level total station was used to measure reef and island topography on 10 across reef transects including the profile used for numerical model analysis. The profiles were combined with RTK-GPS survey points from the reef flat to create a terrain model of the reef flat and shoreline. Shallow water topography data were combined with satellite imagery and single beam echo-sounding data [*Hoeke et al.*, 2014] to create a bathymetry map of the atoll reef flat near Fatato Island (Fig. 1c). All references to topographic elevation are relative to MSL = 0.

The 1D model transect used for wave simulations is a composite of the total station measured island and reef flat profile and the reef slope bathymetry at the instrument transect location (Fig. 1c). The total station profile provided coverage of Fatato Island until the outer reef flat with a seaward limit 1.2 m below MSL, 90 m from the beach toe (Fig. 1d). The transect was extended seaward by overlapping and stitching a profile sliced from the atoll bathymetry that provided 10 m resolution coverage of the outer reef flat, the reef edge and reef slope to the 100 m depth contour (Fig. 1c). Total station and bathymetry data were both referenced to x = 0 m at the toe of beach and interpolated to 1 m resolution for numerical model simulations. The model domain was 1,024 m long, with imported waves propagating for 700 m over a uniform depth of 100 m before reaching the atoll reef profile as indicated by measurements of reef bathymetry and island topography data [*Beetham et al.*, 2016].

3.2 Numerical model

The fully nonlinear Green-Naghdi solver model described in *Popinet* [2015] was used to simulate wave interaction with the reef and island. The model was previously evaluated

against field data from Fatato, achieving model skill > 0.96 for predictions of H_{ss} (significant wave height for the SS band), H_{ig} (significant wave height for the IG band) and setup elevation at the shoreline, across 500 different incident wave and tide combinations [*Beetham et al.*, 2016]. The numerical model has also been validated against a series of benchmark test scenarios for runup and overwash [*Popinet*, 2014, 2015; *Beetham*, 2016]. These scenarios include, runup on a planar beach, runup on a conical island, waves overtopping a sea wall, runup on a coral reef shoreline, overtopping a reef crest and overtopping on a complex shelf with a conical island. The phase-resolving model simulates dispersion using the Green-Naghdi equations and locally switches to a nonlinear shallow water system to represent wave breaking when the free-surface slope exceeds 1 (45°) [*Bonneton et al.*, 2011a; *Popinet*, 2015]. A benefit of this fully nonlinear phase-resolving approach is that no specific parameterization is required to represent surf-zone dynamics associated with IG waves and setup because the model appropriately accounts for momentum balances created by an irregular incident wave field [*Bonneton et al.*, 2010, 2011b]. Similar models have been shown to accurately represent the formation and behavior of IG waves gentle sloping beaches [*Tissier et al.*, 2012] and on coral reefs [*Roeber and Bricker*, 2015; *Shimozono et al.*, 2015].

3.3 Model experiments

3.3.1 Boundary conditions

Model simulations presented here encompass the contemporary spring tidal range (SL = -1.0 m to SL = 1.0 m) and represent a range of SLR magnitudes from 0.05 m to 1.5 m above present spring high (SL = 1.05 m to SL = 2.5 m), relative to MSL = 0. Three non-extreme wave conditions were used, based on analysis of 34 year wave hind-cast data offshore the eastern rim of Funafuti Atoll [*Durrant et al.*, 2014; *Hoeke et al.*, 2014]. Wave conditions include, a) mean significant wave height and period (H_s = 1.3 m; T_s = 10 s), and the average annual-maximum wave heights associated with a) local storm activity (H_s = 2.6 m; T_s = 10 s)

and b) long period swell (H_s = 2.1 m; T_s = 16 s). Measured wave field data offshore Fatato from *Beetham et al.* [2016] were used as a boundary condition to ensure accurate representation of infragravity wave dynamics and setup magnitude. The surface water level time-series representing each wave condition was imported into the offshore model boundary (h = 100 m) to initiate each simulation (Fig. 3). Mean waves were characterized by low energy across a range of frequencies with distinct energy peaks at 0.079 and 0.1 Hz (Fig. 3a). Swell waves had the largest peak in spectral density, centered at 0.06 Hz (Fig. 3b). Storm waves had a lower peak spectral density than swell waves but the wide distribution of high energy centered around 0.95 Hz resulted in the largest gross energy of all wave conditions used in this analysis (Fig. 3c). More information on model calibration and performance for simulating waves on Fatato is available in *Beetham et al.* [2016].

3.3.2 Simulations involving sea-level rise with a static reef response

Assuming no morphological response from the reef or island, across reef wave transformation for each of the three boundary wave conditions was simulated using 71 different sea-levels (213 separate simulations). Sea-level (SL) was increased at 0.05 m increments, from SL = -1 (mean spring low) to SL = 2.5 (mean spring high + 1.5 m).

3.3.3 Simulations involving sea-level rise with a keep-up reef response

The same wave conditions were used to simulate how wave processes will change if the reef flat exhibits a vertical growth response to SLR. Simulations of high, mean, and low tide stages were undertaken for SLR = 0, 0.5, 1 and 1.5 m respectively, and repeated using the two previously described reef response morphologies.

3.4 Model outputs and analysis

Each simulation ran for the 2048 second (~35 minute) duration of the input wave field time-series. This time period ensures that multiple wave groups were represented in each simulation. Only model outputs after 512 s were used to calculate wave and overtopping

statistics to ensure the wave field had fully developed across the reef flat. Time-series data were extracted at 10 Hz at 5 m intervals across the reef flat, with outputs at the shoreline sensor (0.38 m below MSL) and the berm crest (MSL + 3.5 m) the main focus of this analysis (Fig. 1d). A 0.04 Hz band pass filter was used to separate high and low frequency waves and the zero down-crossing method was used to quantify significant wave height for sea-swell waves (H_{ss}) and infragravity waves (H_{ig}). Power spectral density (PSD) calculations from the raw time-series were used to quantify total spectral density within the wave field (0.0037-2 Hz), total spectral density within the SS wave band (0.04-2 Hz) and total spectral density within the IG wave band (0.0037-0.04 Hz). Wave overtopping events were identified and OW rates were calculated using time-series data extracted from the berm crest (Fig. 1d). OW rate is presented as the mean volume of water passing over the berm during the final 1,536 seconds (~25 minutes) of each simulation and is measured in cubic meters per second, assuming the model represents a 1 m wide section of the island. Significant levels of overwash can result in the central island basin filling with water, however this does not interfere with calculated OW rates on the ocean berm because drainage occurs on the lower elevation leeward island ridge.

4. Results

4.1 Sea-level rise with a static reef response

4.1.1 Shoreline wave processes

Model simulations with a static reef morphology indicate that a fundamental shift in the shoreline process regime will occur on reefs that exhibit no morphological adjustment to future SLR (Fig. 4). First, model results demonstrate a near linear increase in SS wave height (H_{ss}) at the shoreline as sea-level increases from spring low tide (SL = -1.0 m) to spring high tide (SL = 1 m), with continued increase in H_{ss} towards SL = 2.5 m, encompassing SLR scenarios between 0.05 and 1.5 m above the contemporary tidal range (Fig. 4a-c). The

positive relationship between wave height and reef depth is accompanied by a near exponential decrease in setup elevation at the shoreline, as less energy is dissipated through wave breaking and friction (Fig. 4a-c). The relationship between shoreline IG wave height (H_{ig}) and SLR is more complex (Fig. 4d-f). Under each wave condition H_{ig} initially increased as reef water depth increased from SL = -1 m, but maximum H_{ig} was observed within the current tidal range, at SL = 0 m, 0.35 m and 0.65 m for mean, swell and storm waves respectively (Fig. 4g-i). Beyond these maximum values, H_{ig} decreased as sea-level increased towards current spring high tide and beyond present levels (Fig. 4). Model outputs show that an inert reef response to rising sea-level will shift the wave environment at island shorelines from one currently dominated by IG energy to a regime where incident frequency SS waves are the primary source of hydrodynamic interaction with island shorelines (Fig. 4d-f). Indeed, model outputs show a marked increase in net shoreline wave energy once SS waves accounted for more than 50% of shoreline energy (Fig. 4g-i). This threshold sea-level threshold for SS waves becoming the dominant source of energy is reached around high tide under mean wave conditions and at low levels of SLR for swell and storm waves respectively (Fig. 4).

4.1.2 Wave overtopping

Importantly, model results show that wave overtopping of the island shoreline does not occur within the contemporary tidal range under annual-maximum storm or swell conditions (Fig. 4j-l). Larger wave events associated with decadal to centennial scale return periods are capable of overtopping islands on Funafuti Atoll (e.g. Cyclone Bebe in 1972), but this study focused on modal wave conditions that if capable of overtopping islands may significantly compromise permanent habitation [*Storlazzi et al.*, 2015]. Island overtopping under the annual storm and swell conditions used in this study initially occur at spring high tide with SLR = 0.3 m and 0.35 m, respectively (SL = 1.3 m and 1.35 m). A threshold sea-level of 1.9

m above MSL (spring high tide plus 0.9 m of SLR) is required for island overtopping under mean wave conditions. Once the SL threshold was reached for each wave condition, overwash (OW) volume increased exponentially, and overtopping moved from a single wave surge (OW < 0.003 m^3/s) toward multiple wave groups (OW > 0.05 m^3/s) breaching the berm (Fig. 4j-l). Unlike contemporary observations of overtopping, model outputs identify SS waves will provide the primary source of overwash flow with SLR, under non-extreme wave. Notably, swash motions generated by IG waves are capable of surging landward with considerable momentum and significantly exceed the reach of SS waves [*Guza and Thornton*, 1982]. Therefore, SS wave driven overtopping on reef islands at higher sea-levels under non-extreme waves will be fundamentally different to the IG dominated and destructive overtopping events observed during extreme wave conditions at contemporary sea-level [*Roeber and Bricker*, 2015; *Cheriton et al.*, 2016].

4.2 Effectiveness of vertical reef accretion at protecting reef islands

4.2.1 Shoreline wave processes

Wave processes at the shoreline associated with SLR and vertical reef adjustment are not identical to contemporary conditions because the reef flat is currently elevated 0.3 m above spring low tide compared to the adjusted reefs being level with spring low tide. However, model simulations representing vertical reef accretion do indicate that much of the projected increase in shoreline wave energy can be mitigated through natural reef morphology feedbacks (Fig. 5). SS wave height at high tide remained within 10% and 5% of contemporary high tide values for simulations with outer reef accretion and full reef accretion, respectively. In comparison, SS wave height at high tide increased by 20% for every 0.5 m of SLR when the reef remained static (Fig. 5). The contemporary reef is effective at dissipating 54.6% of incident wave height at high tide, when averaged across the three wave conditions. Reef accretion maintains this same magnitude of dissipation. In comparison,

a static reef response is associated with 30% and 40% less wave dissipation at SLR = 1.0 m and 1.5 m, respectively. Averaged across all simulated wave conditions and tidal stages (low, mean, high), vertical accretion of the outer reef flat was effective at offsetting 15-57% of the increase in SS wave height associated with a static response to SLR, depending on the SLR magnitude (Fig. 5). Comparatively, full reef flat accretion was capable of dampening the SLR associated increase in SS wave height by 33-79%.

Both accretionary morphologies resulted in larger IG waves at the shoreline under each SLR scenario when compared to SLR and a static reef morphology (Fig. 5; Table S1). IG wave heights associated with both reef accretion morphologies remained within 10% of contemporary magnitudes at high tide, on average, with a slight decrease in height due to the contemporary reef being intertidal (Fig. 5d-f). In contrast, SLR with a static reef morphology resulted in a dramatic reduction in shoreline IG wave height, with a 10% decrease in height associated with every 0.5 m increase in sea level. Model outputs also show that SLR will result in larger IG wave heights impacting atoll islands at low tide and mid tide, regardless of reef response morphology or wave condition (Table S1).

An inert reef response to SLR resulted in setup decreasing at mid and high tide, with an increase in setup only observed at low tide under conditions when the shoreline was previously dry. Reef accretion resulted in similar setup magnitudes to contemporary conditions with setup 54-60% larger than the static reef morphology for outer and full reef accretion, respectively (Fig. 5).

4.2.2 Wave overtopping

Model results show that a vertical growth response to SLR is effective at decreasing overwash volume, given the assumption that island morphology remains static in all simulations (Fig. 5). However, model outputs also show that reef accretion has limited potential to prevent overtopping or offset the SLR threshold when overwash occurs for a

particular wave condition. For storm waves, outer reef accretion reduced OW volume by 46% on average, increasing to 65% reduction with full reef flat development (Fig. 5; Table S2). Reef growth was less effective at preventing overtopping under swell conditions, with OW volume reduced by 27% and 57% for outer and full reef growth morphologies, respectively (Table S2). Reef growth was most effective at decreasing OW under mean wave conditions, with an average reduction of 78% and 93%, respectively. Overall, an accretionary response to SLR will substantially reduce the magnitude of OW when compared to a static response. However, model results emphasize that future reef growth has minimal influence on preventing the occurrence of wave overtopping with SLR and highlight that reef accretion has limited potential to offset the SL threshold when overtopping first occurs (Fig. 6).

5. Discussion

Previous studies on the impacts of SLR on reef island flooding are based on the assumption that reef morphology will remain static and exhibits no structural adjustment to SLR [*Storlazzi et al.*, 2015]. Despite the multiple and compounding stressors that will likely limit future reef growth [*Anthony et al.*, 2011; *Hoegh-Guldberg et al.*, 2017; *Hughes et al.*, 2017], recent field assessments have measured vertical reef accretion in response to relative or absolute SLR [*Brown et al.*, 2011; *Scopélitis et al.*, 2011; *Saunders et al.*, 2015; *van Woesik et al.*, 2015]. Model based projections from field data in the western Pacific [*van Woesik et al.*, 2015] suggest that some reefs can potentially keep-up with future SLR forced by RPC4.5 (6.1 mm/yr) but will likely lag behind RPC6.0 scenarios (7.4 mm/yr), with limited potential for a keep-up reef response under RPC8.5 (11.2 mm/yr). Previous hydrodynamic studies have also relied on phase-averaged models that do not adequately resolve infragravity wave processes, setup, runup and overwash motions [*Roeber and Bricker*, 2015]. These secondary surf-zone processes provide a primary contribution to runup [*Beetham et al.*, 2016] and inundation [*Cheriton et al.*, 2016] on atoll islands. Results presented here offer unique and

comprehensive insight on how SLR will change the full spectrum of wave processes that contribute to island flooding and provide the first assessment regarding how effective future reef growth is at mitigating adverse effects of SLR. Consistent with previous studies, SLR with no reef-adjustment will increase reef depth and allow larger waves within the SS frequency band to impact reef island shorelines. However, model results from Funafuti also show that as sea-level increases and more energy is retained within the SS frequency band, less energy is transferred into the IG wave band. Model results identify that shoreline wave energy transitions from being IG dominant to being SS dominant when reef submergence reaches a critical threshold of $H_o/h_r < 1.3$ (where h_r is depth at the reef edge). Our findings contrast previous studies that predict an increase in IG wave height with SLR because of the associated decrease in bottom friction [*Quataert et al.*, 2015]. These contrasting results may be associated with differing reef widths or the way different models represent nonlinear interactions between SS and IG waves. Similar to IG waves, setup water level on coral reefs will decrease with SLR, as presented here and previously predicted using empirical data [*Becker et al.*, 2014].

A significant advantage of fully nonlinear phase-resolving models is that the free-surface boundary condition can directly simulate runup and overtopping flow. Previous wave modeling based studies of flooding on atoll islands have relied on modified runup equations based on shoreline wave height to predict flooding magnitudes [*Quataert et al.*, 2015; *Storlazzi et al.*, 2015]. Another limitation of previous research that remains unresolved in this study is the unknown morphological response of atoll islands to SLR. Previous research on the potential for islands to adjust their morphology in response to SLR are limited in number and scope, but there is a hypothesis that some islands will accrete vertically and migrate lagoon-ward as overwash processes re-work new and existing island sediment [*Cowell and Kench*, 2001; *Kench and Cowell*, 2001]. All results in this study assume no island adjustment

to SLR and therefore overtopping values do not account for how overtopping events may result in changes to the shoreline position and elevation. To justify this omission we argue that the dramatic change in island morphology required to sustain island elevation above rising sea levels will itself compromise ongoing habitation on atoll islands.

With a static reef and island response to SLR, overtopping under annual conditions will initially occur on the eastern rim of Funafuti at spring high tide with 0.3 m of SLR. Overtopping under annual-maximum wave events will occur within four decades if the current rate of SLR (5.1 mm/yr) prevails or within two decades if emissions continue to increase under IPCC *business-as-usual* projections (Table 1). Model outputs for storm and swell waves show that overwash between SLR = 0.3 and 0.85 m is associated with 2 or 3 waves overtopping the berm in a 35 minute burst, resulting in low volumes of flooding that are potentially manageable for island communities. Under these annual-maximum conditions, spring high tide overwash volume increases substantially when SLR exceeds 0.9 m, as multiple wave groups are able to breach the island berm, causing a significant increase in flood volume. The threshold for wave generated flooding to occur under mean wave condition at spring high tide was also SLR = 0.9 m (Fig. 4), highlighting this as a conservative tipping-point for the frequency and magnitude of wave generated flooding to overwhelm recovery potential. Mild overtopping by mean waves and serious overtopping from annual-maximum events (SLR = 0.9 m) will occur by 2090 under *business-as-usual* SLR projections, and will seriously strain the resilience of inhabited reef islands. The change in hydrodynamic boundary conditions at island shorelines will likely result in significant shoreline change on natural atoll islands over the next 70 years, while significant flooding will occur on islands with urbanized shorelines. Based on IPCC rates of SLR under lower emission scenarios, the onset of serious wave driven flooding can be significantly delayed if global action is taken to reduce emissions (Table 1). Under modal wave conditions,

overtopping with SLR will be driven by incident frequency SS waves and not long period infragravity waves, which are consistently identified as the primary driver of overtopping and destructive flooding on reef shorelines [*Roeber and Bricker*, 2015; *Cheriton et al.*, 2016].

Model outputs show that future reef accretion will effectively preserve the contemporary tidal modulation of wave processes at the shoreline and will significantly mitigate wave flooding magnitudes. The inability of reef accretion to prevent overtopping is partly attributed to IG waves and setup compensating for the reduction in SS wave height achieved by reef accretion, but also relates to the fact that SLR decreases island elevation above the still water level and therefore lowers the threshold energy required for overtopping. Even though vertical reef growth cannot prevent overtopping, the effectiveness in offsetting a rise in shoreline energy and significantly decreasing overwash volume provides substantial support for active coral reef restoration [*Clark and Edwards*, 1999; *Temmerman et al.*, 2013; *Rinkevich*, 2014] as a source of '*cost-effective*' shoreline protection for island communities facing SLR [*Ferrario et al.*, 2014].

Our results, elucidating changes in the full wave spectrum impacting shorelines and consequences for island overtopping, are critical for resolving the changing hazard-scape of islands and their ongoing habitability. However, reef islands are dynamic features that adjust their shoreline morphology in response to environmental variability across a range of temporal scales [*McLean and Kench*, 2015] and future work is required to address the morphological adjustment of islands to SLR. However, the assumption of a static shoreline in this study provides a baseline 'worst case' assessment of the increasing exposure of island communities to wave hazards associated with increasing sea-level. Further, morphologic change on many developed islands is compromised by development pressure, environmental degradation, and histories of hard engineering [*McLean and Kench*, 2015]. Communities on urbanized islands will be confronted with significant adaptation challenges over the next half

century if no action is taken to offset the current trajectory of climate change driven sea-level rise.

Acknowledgements

This research was undertaken while Edward Beetham was being supported by a University of Auckland Doctoral Scholarship. All data associated with this research (including numerical model simulation files, input files and raw output files) are publically available from the Figshare repository doi: 10.17608/k6.auckland.5150140, url: https://figshare.com/s/eedcf0b1a8ab1b2b103a. The Green Naghdi solver used in this research is part of Basilisk and is freely available online at basilisk.fr.

References

Anthony, K. R. N., J. A. Maynard, G. Diaz-Pulido, P. J. Mumby, P. A. Marshall, L. Cao, and O. V. E. Hoegh-Guldberg (2011), Ocean acidification and warming will lower coral reef resilience, *Glob. Chang. Biol.*, *17*, 1798–1808, doi:10.1111/j.1365-2486.2010.02364.x.

Aronson, R. B., and W. F. Precht (2016), Physical and Biological Drivers of Coral-Reef Dynamics, in *Coral Reefs at the Crossroads*, edited by D. K. Hubbard, C. S. Rogers, J. H. Lipps, and J. G. D. Stanley, pp. 261–275, Springer Netherlands, Dordrecht.

Barnett, J., and W. N. Adger (2003), Climate Dangers and Atoll Countries, *Clim. Change*, *61*, 321–337, doi:10.1023/B:CLIM.0000004559.08755.88.

Becker, J., M. Merrifield, and M. Ford (2014), Water level effects on breaking wave setup for Pacific Island fringing reefs, *J. Geophys. Res. Ocean.*, *119*, 914–932, doi:10.1002/2013JC009373.

Becker, M., B. Meyssignac, C. Letetrel, W. Llovel, A. Cazenave, and T. Delcroix (2012), Sea level variations at tropical Pacific islands since 1950, *Glob. Planet. Change*, *80–81*, 85–98, doi:http://dx.doi.org/10.1016/j.gloplacha.2011.09.004.

Beetham, E. P. (2016), Field and numerical investigations of wave transformation and inundation on atoll islands, Ph.D thesis, 206 pp., University of Auckland, New Zealand, doi: http://hdl.handle.net/2292/29852.

Beetham, E. P., P. S. Kench, J. O'Callaghan, and S. Popinet (2016), Wave transformation and shoreline water level on Funafuti Atoll, Tuvalu, *J. Geophys. Res. Ocean.*, 121, 311–326.

Bonneton, *P., N. Bruneau, B. Castelle,* and F. Marche (2010), Large-Scale Vorticity Generation Due to Dissipating Waves in the Surf Zone, *Discret. Contin. Dyn. Syst. B*, 13, 729–738, doi:10.3934/dcdsb.2010.13.729.

Bonneton, P., F. Chazel, D. Lannes, F. Marche, and M. Tissier (2011a), A splitting approach for the fully nonlinear and weakly dispersive Green–Naghdi model, *J. Comput. Phys.*, 230, 1479–1498, doi:http://dx.doi.org/10.1016/j.jcp.2010.11.015.

Bonneton, P., E. Barthelemy, F. Chazel, R. Cienfuegos, D. Lannes, F. Marche, and M. Tissier (2011b), Recent advances in Serre-Green Naghdi modelling for wave transformation,

breaking and runup processes, *Eur. J. Mech. B-Fluids*, 30, 589–597, doi:10.1016/j.euromechflu.2011.02.005.

Brown, B. E., R. P. Dunne, N. Phongsuwan, and P. J. Somerfield (2011), Increased sea level promotes coral cover on shallow reef flats in the Andaman Sea, eastern Indian Ocean, *Coral Reefs*, 30, 867–878, doi:10.1007/s00338-011-0804-9.

Cheriton, O., C. D. Storlazzi, and K. Rosenberger (2016), Observations of wave transformation over a fringing coral reef and the importance of low-frequency waves and offshore water levels to runup, overwash, and coastal flooding, *J. Geophys. Res. Ocean.*, 121, 3121–3140, doi:10.1002/2015JC011231.

Church, J. A., P. U. Clark, A. Cazenave, J. M. Gregory, S. Jevrejeva, A. Levermann, M. A. Merrifield, G. A. Milne, R. S. Nerem, and P. D. Nunn (2013), Sea level change, in Climate Change 2013: The Physical Science Basis. *Contribution of Working Group I to the Fifth Assessment Report of the Intergovernmental Panel on Climate Change, edited by T. Stocker, D. Qin, G. Plattner, M. T*ignor, S. Allen, J. Boschung, A. Nauels, Y. Xia, V. Bex, and P. M. Midgley, pp. 1137–1216, Cambridge University Press, Cambridge, United Kingdom.

Clark, S., and A. J. Edwards (1999), An evaluation of artificial reef structures as tools for marine habitat rehabilitation in the Maldives, *Aquat. Conserv. Mar. Freshw. Ecosyst.*, 9, 5–21, doi:10.1002/(SICI)1099-0755(199901/02)9:1<5::AID-AQC330>3.0.CO;2-U.

Connell, J. (2003), Losing ground? Tuvalu, the greenhouse effect and the garbage can, *Asia Pac. Viewp.,* 44, 89–107, doi:10.1111/1467-8373.00187.

Cowell, P. J., and P. S. Kench (2001), The morphological response of atoll islands to sea-level rise. Part 1: modifications to the shoreface translation model, *J. Coast. Res.*, 633–644.

Durrant, T., D. Greenslade, M. Hemer, and C. Trenham (2014), A global wave hindcast focussed on the Central and South Pacific, *CAWCR Tech. Rep. 070,* Bureau of Meteorology, Melbourne, Australia.

Farbotko, C., and H. Lazrus (2012), The first climate refugees? Contesting global narratives of climate change in Tuvalu, *Glob. Environ. Chang.*, 22, 382–390, doi:http://dx.doi.org/10.1016/j.gloenvcha.2011.11.014.

Ferrario, F., M. W. Beck, C. D. Storlazzi, F. Micheli, C. C. Shepard, and L. Airoldi (2014), The effectiveness of coral reefs for coastal hazard risk reduction and adaptation, *Nat. Commun.,* 5, doi:10.1038/ncomms4794.

Guilcher, A. (1988), *Coral reef geomorphology*., 228 pp., Wiley, New York.

Guza, R. T., and E. B. Thornton (1982), Swash oscillations on a natural beach, *J. Geophys. Res. Ocean.*, 87, 483–491, doi:10.1029/JC087iC01p00483.

Hamylton, S. M., J. X. Leon, M. I. Saunders, and C. D. Woodroffe (2014), Simulating reef response to sea-level rise at Lizard Island: A geospatial approach, *Geomorphology*, 222, 151–161, doi:http://dx.doi.org/10.1016/j.geomorph.2014.03.006.

Hoegh-Guldberg, O. (2014), Coral reef sustainability through adaptation: glimmer of hope or persistent mirage?, *Curr. Opin. Environ. Sustain.*, 7, 127–133, doi:http://dx.doi.org/10.1016/j.cosust.2014.01.005.

Hoegh-Guldberg, O. et al. (2007), Coral Reefs Under Rapid Climate Change and Ocean Acidification, *Science* (80)., 318, 1737–1742, doi:10.1126/science.1152509.

Hoegh-Guldberg, O., E. S. Poloczanska, W. Skirving, and S. Dove (2017), Coral Reef Ecosystems under Climate Change and Ocean Acidification, *Front. Mar. Sci.*, 4, 158, doi:10.3389/fmars.2017.00158.

Hoeke, R., K. McInnes, and J. O'Grady (2014), Downscaling wave climate at a Funafuti, Tuvalu, *Report, Cent. for Aust. Weather and Clim. Res.*, Melbourne, Australia.

Hopley, D. (2011), Climate Change: impact of sea level rise on reef flat zonation and productivity, in *Encyclopedia of Modern Coral Reefs Structure, Form and Process,* edited by D. Hopley, pp. 210–214, Springer, Dordrecht, The Netherlands.

Hughes, T. P. et al. (2003), Climate Change, Human Impacts, and the Resilience of Coral Reefs, *Science* (80)., 301, 929–933, doi:10.1126/science.1085046.

Hughes, T. P., N. A. J. Graham, J. B. C. Jackson, P. J. Mumby, and R. S. Steneck (2010), Rising to the challenge of sustaining coral reef resilience, *Trends Ecol. Evol.*, 25, 633–642, doi:http://dx.doi.org/10.1016/j.tree.2010.07.011.

Hughes, T. P. et al. (2017), Coral reefs in the Anthropocene, *Nature*, 546(7656), 82–90.

Jackson, J. B. C. et al. (2001), Historical Overfishing and the Recent Collapse of Coastal Ecosystems, *Science* (80)., 293, 629–637, doi:10.1126/science.1059199.

Kench, P. S., and P. J. Cowell (2001), The morphological response of atoll islands to sea-level rise. Part 2: application of the modified shoreface translation model (STM), *J. Coast. Res.*, 645–656.

Kench, P. S., C. T. Perry, and T. C. N.-G. G. . G. 2009 (LC) Spencer (2009), Coral Reefs, in *Geomorphology and global environmental change*, edited by O. Slaymaker, T. Spencer, and C. Embleton-Hamann, pp. 182–213, Cambridge University Press, Cambridge ; New York.

Kench, P. S., D. Thompson, M. R. Ford, H. Ogawa, and R. F. McLean (2015), Coral islands defy sea-level rise over the past century: Records from a central Pacific atoll, *Geology*, 43, 515–518.

Lazrus, H. (2012), Sea Change: Island Communities and Climate Change, *Annu. Rev. Anthropol.*, 41, 285–301, doi:10.1146/annurev-anthro-092611-145730.

Lin, C. C., C. R. Ho, and Y. H. Cheng (2014), Interpreting and analyzing King Tide in Tuvalu, *Nat. Hazards Earth Syst. Sci.*, 14, 209–217, doi:10.5194/nhess-14-209-2014.

Longuet-Higgins, M. S., and R. W. Stewart (1962), Radiation stress and mass transport in gravity waves, with application to "surf beats," *J. Fluid Mech.*, 13, 481–504.

Masselink, G. (1995), Group bound long waves as a source of infragravity energy in the surf zone, *Cont. Shelf Res.*, 15, 1525–1547, doi:http://dx.doi.org/10.1016/0278-4343(95)00037-2.

McCubbin, S., B. Smit, and T. Pearce (2015), Where does climate fit? Vulnerability to climate change in the context of multiple stressors in Funafuti, *Tuvalu, Glob. Environ. Chang.*, 30, 43–55, doi:http://dx.doi.org/10.1016/j.gloenvcha.2014.10.007.

McLean, R., and P. S. Kench (2015), Destruction or persistence of coral atoll islands in the face of 20th and 21st century sea-level rise?, *Wiley Interdiscip. Rev. Clim. Chang.*, doi:10.1002/wcc.350.

Merrifield, M., J. Becker, M. Ford, and Y. Yao (2014), Observations and estimates of wave-driven water level extremes at the Marshall Islands, *Geophys. Res. Lett.*, 41, 7245–7253, doi:10.1002/2014GL061005.

Nurse, L. A., R. F. Mclean, J. Agard, L. P. Briguglio, V. Duvat-Magnan, N. Pelsikoti, E. TompkinsS, and A. Webb (2014), Small islands, *Clim. Chang. 2014 Impacts, Adapt. Vulnerability. Part B Reg. Asp. Contrib. Work. Gr. II to Fifth Assess. Rep. Intergov. Panel Clim. Chang.*, 1613–1654.

Ohde, S., M. Greaves, T. Masuzawa, H. A. Buckley, R. Van Woesik, P. A. Wilson, P. A. Pirazzoli, and H. Elderfield (2002), The chronology of Funafuti Atoll: revisiting an old friend, *Proc. R. Soc. London A Math. Phys. Eng. Sci.*, 458, 2289–2306, doi:10.1098/rspa.2002.0978.

Patel, S. S. (2006), Climate science: A sinking feeling, *Nature*, 440, 734–736.

Péquignet, A. C., J. M. Becker, and M. A. Merrifield (2014), Energy transfer between wind waves and low-frequency oscillations on a fringing reef, Ipan, Guam, *J. Geophys. Res. Ocean.*, 119, 6709–6724, doi:10.1002/2014JC010179.

Perry, C. T., E. N. Edinger, P. S. Kench, G. N. Murphy, S. G. Smithers, R. S. Steneck, and P. J. Mumby (2012), Estimating rates of biologically driven coral reef framework production and erosion: a new census-based carbonate budget methodology and applications to the reefs of Bonaire, *Coral Reefs*, 31, 853–868, doi:DOI 10.1007/s00338-012-0901-4.

Perry, C. T., G. N. Murphy, N. A. J. Graham, S. K. Wilson, F. A. Januchowski-Hartley, and H. K. East (2015), Remote coral reefs can sustain high growth potential and may match future sea-level trends, *Sci. Rep.*, 5.

Popinet, S. (2014), A solver for the Green-Naghdi equations, http://www.basilisk.fr/src/green-naghdi.h, 2014.

Popinet, S. (2015), A quadtree-adaptive multigrid solver for the Serre–Green–Naghdi equations, *J. Comput. Phys.*, 302, 336–358, doi:http://dx.doi.org/10.1016/j.jcp.2015.09.009.

Quataert, E., C. Storlazzi, A. van Rooijen, O. Cheriton, and A. van Dongeren (2015), The influence of coral reefs and climate change on wave-driven flooding of tropical coastlines, *Geophys. Res. Lett.*, doi:10.1002/2015GL064861.

Rinkevich, B. (2014), Rebuilding coral reefs: does active reef restoration lead to sustainable reefs?, *Curr. Opin. Environ. Sustain.*, 7, 28–36, doi:http://dx.doi.org/10.1016/j.cosust.2013.11.018.

Roeber, V., and J. D. Bricker (2015), Destructive tsunami-like wave generated by surf beat over a coral reef during Typhoon Haiyan, *Nat. Commun.*, 6, doi:10.1038/ncomms8854.

Roeber, V., and K. F. Cheung (2012), Boussinesq-type model for energetic breaking waves in fringing reef environments, *Coast. Eng.*, 70, 1–20.

Saunders, M., S. Albert, C. Roelfsema, J. Leon, C. Woodroffe, S. Phinn, and P. Mumby (2015), Tectonic subsidence provides insight into possible coral reef futures under rapid sea-level rise, *Coral Reefs*, 1–13, doi:10.1007/s00338-015-1365-0.

Scopélitis, J., S. Andréfouët, S. Phinn, T. Done, and P. Chabanet (2011), Coral colonisation of a shallow reef flat in response to rising sea level: quantification from 35 years of remote sensing data at Heron Island, Australia, *Coral Reefs*, 30, 951–965, doi:10.1007/s00338-011-0774-y.

Sheppard, C., D. J. Dixon, M. Gourlay, A. Sheppard, and R. Payet (2005), Coral mortality increases wave energy reaching shores protected by reef flats: Examples from the Seychelles, *Estuar. Coast. Shelf Sci.*, 64, 223–234, doi:10.1016/j.ecss.2005.02.016.

Shimozono, T., Y. Tajima, A. B. Kennedy, H. Nobuoka, J. Sasaki, and S. Sato (2015), Combined infragravity wave and sea-swell runup over fringing reefs by super typhoon Haiyan, *J. Geophys. Res. Ocean.*, doi:10.1002/2015JC010760.

Storlazzi, C. D., E. P. L. Elias, and P. Berkowitz (2015), Many Atolls May be Uninhabitable Within Decades Due to Climate Change, *Sci. Rep.*, 5, 14546, doi:10.1038/srep14546.

Symonds, G., D. A. Huntley, and A. J. Bowen (1982), Two-dimensional surf beat: Long wave generation by a time-varying breakpoint, *J. Geophys. Res. Ocean.*, 87, 492–498, doi:10.1029/JC087iC01p00492.

Temmerman, S., P. Meire, T. J. Bouma, P. M. J. Herman, T. Ysebaert, and H. J. De Vriend (2013), Ecosystem-based coastal defence in the face of global change, *Nature*, 504, 79–83, doi:10.1038/nature12859.

Tissier, M., P. Bonneton, B. Ruessink, F. Marche, F. Chazel, and D. Lannes (2012), Fully nonlinear Boussinesq-type modelling of infragravity wave transformation over a low-sloping beach, *Proc. 33rd Int. Conf. Coast. Eng.*, 33.

van Woesik, R., Y. Golbuu, and G. Roff (2015), Keep up or drown: adjustment of western Pacific coral reefs to sea-level rise in the 21st century, *Open Sci.*, 2, doi:10.1098/rsos.150181.

Woodroffe, C. D. (2008), Reef-island topography and the vulnerability of atolls to sea-level rise, *Glob. Planet. Change*, 62, 77–96, doi:10.1016/j.gloplacha.2007.11.001.

Woodroffe, C. D., and J. M. Webster (2014), Coral reefs and sea-level change, *Mar. Geol.*, 352, 248–267, doi:http://dx.doi.org/10.1016/j.margeo.2013.12.006.

Tables

Table 1: First year associated with overtopping at spring high tide under each simulated wave condition, assuming the reef and island undergo no morphological adjustment to SLR. A range of SLR rates are presented, based on measurements form the instrumental record [*Becker et al.*, 2012] and various IPCC regional concentration pathways [*Church et al.*, 2013].

Scenario	linear SLR rate (mm/yr)	Annual storm event (OWSL=1.3m)	Annual swell event (OWSL=1.35m)	Mean waves (OWSL=1.9m)
IPCC 'Business-as-usual' scenarios [Church et al., 2013]				
RCP8.5 (upper limit)	15.7	2025	2028	2063
RCP8.5 (mean)	11.2	2030	2035	2093
IPCC Reduced emissions scenarios [Church et al., 2013]				
SRES A1B (mean)	8.1	2038	2044	2112
RCP6.0 (mean)	7.4	2040	2047	2121
RCP4.5 (mean)	6.1	2047	2055	2145
RCC2.6 (mean)	4.4	2061	2072	2197
RCP2.6 (lower limit)	2	2121	2146	2421
Instrumental record 1950-2010 [Becker et al., 2012]				
mean rate	5.1	2054	2064	2171

Figure captions

Figure 1: Field setting. a) Location of Funafuti Atoll in the Pacific Ocean. b) Location of Fatato Island on the south facing rim of Funafuti Atoll. c) Outline of Fatato Island with triangles indicating the location of field instruments used for model evaluation [*Beetham et al.*, 2016]. d) Reef and island morphology used in model simulations highlighting where wave data were analysed at the shoreline sensor and where overwash (OW) was quantified.

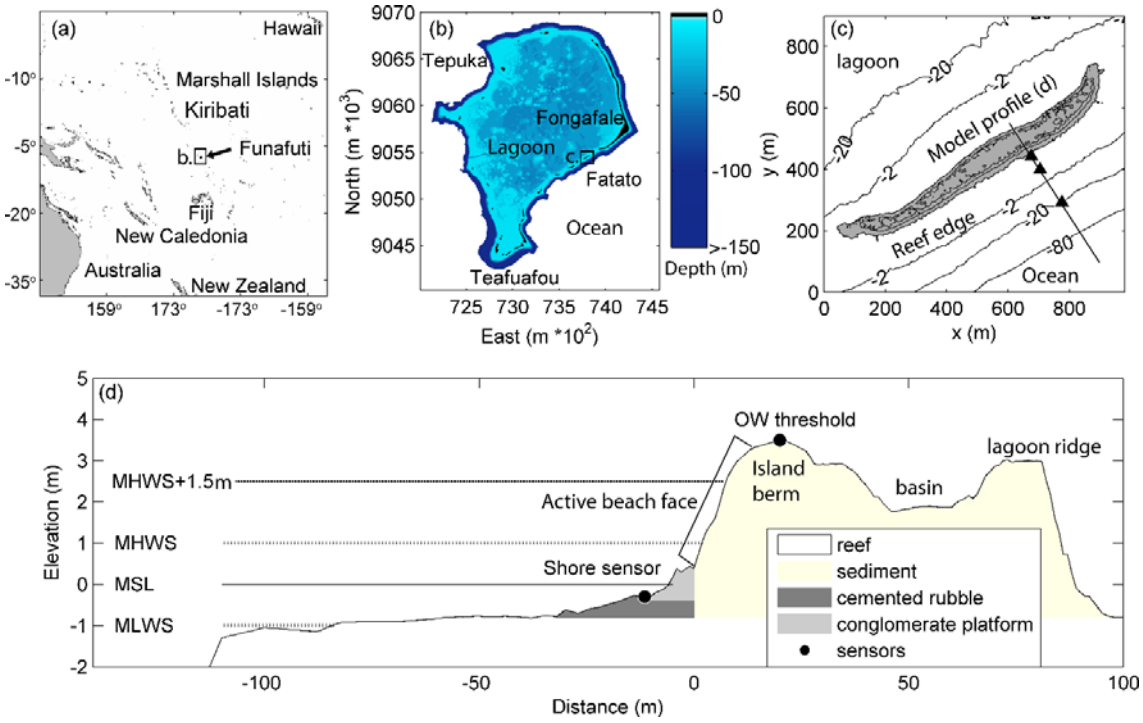

Figure 2: a) Comtemporary reef morphology. b-d) Hypothetical reef growth morphologies used to investigate wave transformation processes and overtopping under different magnitudes of SLR, with reference to adjusted mean low water spring (MLWS) and mean high water spring (MHWS).

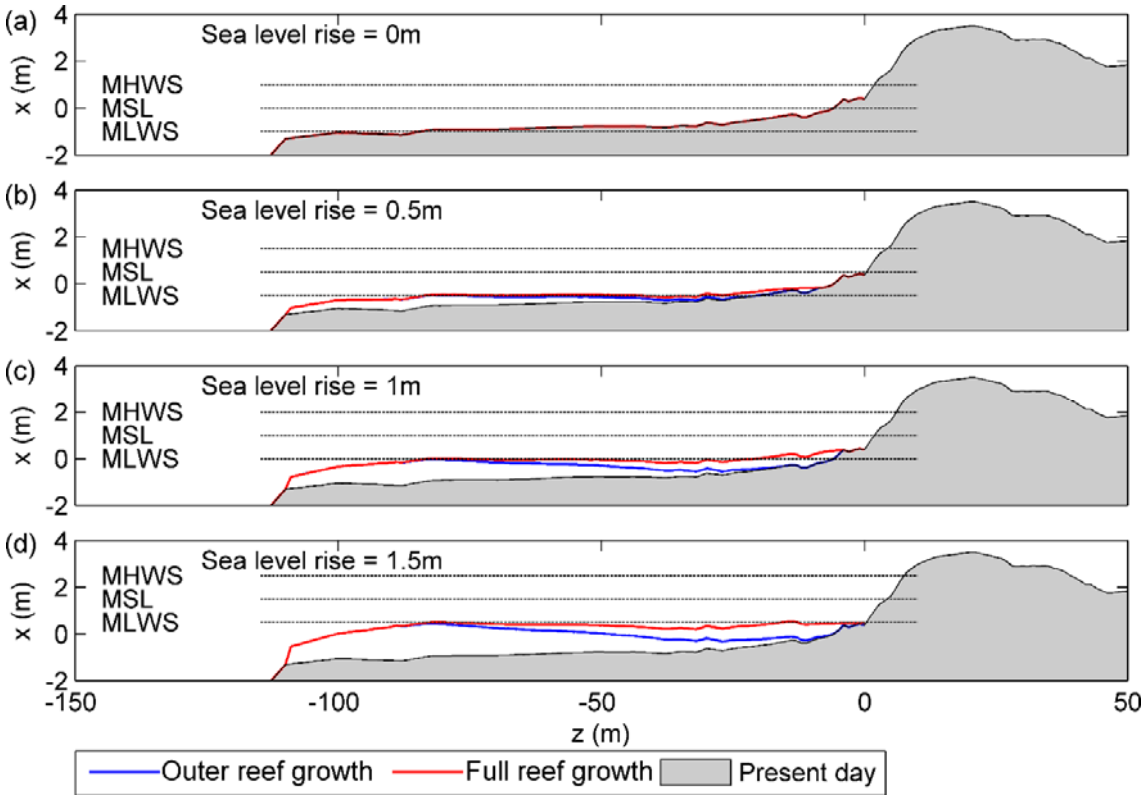

Figure 3: Boundary wave conditions. a-c) Pressure signal and d-f) spectral composition for the mean (H_s = 1.3 m; T_s=10s), swell (H_s = 2.1 m; T_s = 16 s) and storm (H_s = 2.6 m; T_s = 10 s) conditions used in model simulations.

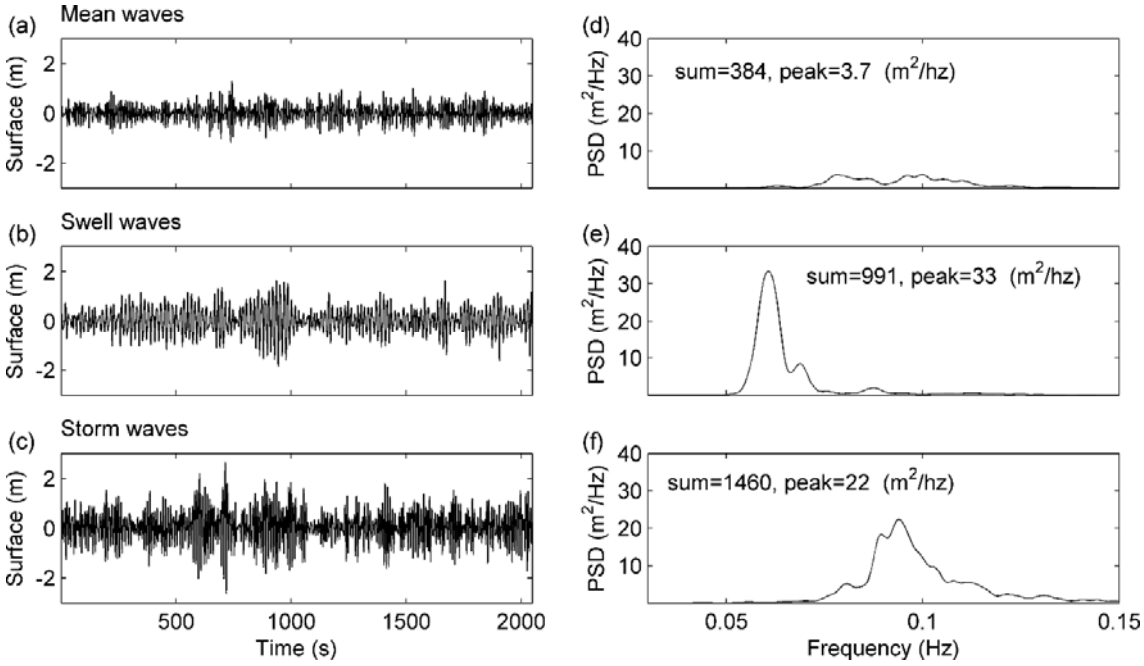

Figure 4: Impact of sea-level rise with a static reef response on shoreline wave processes and overtopping under mean (left), swell (centre) and storm (right) wave conditions, with higher than present sea-levels shaded in light grey. a-c) SS wave height (including line gradient), IG wave height and setup responses to SLR. d-f) Change in absolute power spectral density (PSD) within the SS wave band, IG wave band and net wave field at the shoreline. g-i) Relative contribution of SS wave energy and IG energy to net spectral density at the shoreline with SLR. j-l) Rate of wave overwash (OW) across the island berm, with the overwash sea-level threshold (OWSL) shaded in dark grey.

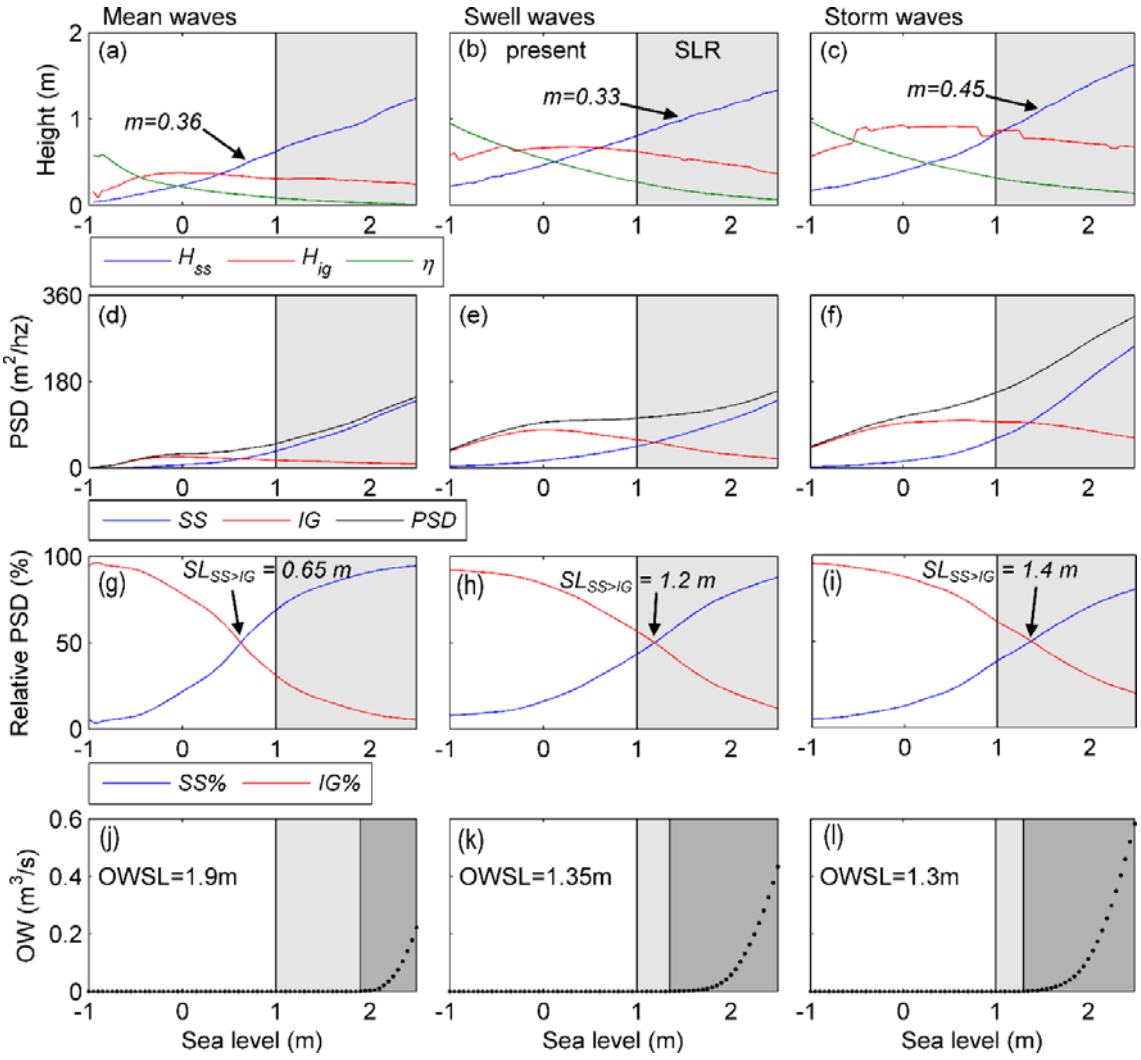

Figure 5: Comparison between wave processes at the shoreline at high tide under static and reef-acction responses to SLR. a-c) sea-swell wave height (H_{ss}), d-f) infragravity wave height (H_{ig}) and g-i) setup ($\overline{\eta}$) and j-l) overwash discharge (OW).

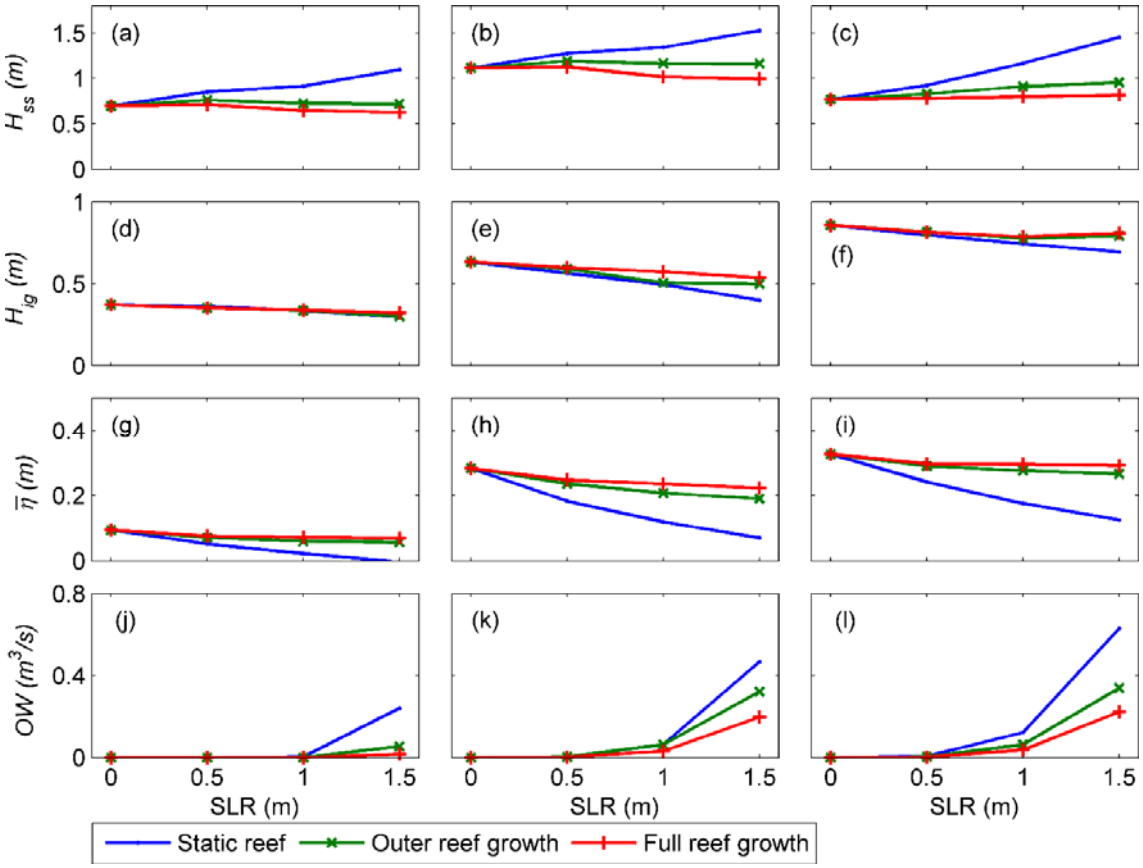

Figure 6: Snapshot model outputs showing free-surface water-level at high tide for different SLR scenarios, with different reef response morphologies (left to right) when the largest OW event occurred under storm wave conditions.